Developmental Cell
Article

Stimulation of Endocytosis and Actin Dynamics by Oskar Polarizes the *Drosophila* Oocyte

Nathalie Vanzo,[1,2] Adrian Oprins,[3] Despina Xanthakis,[3] Anne Ephrussi,[2,*] and Catherine Rabouille[3,*]
[1] Centre de Biologie du Développement, UMR 5547 CNRS/UPS, 118 Rte de Narbonne, 31062 Toulouse Cedex 04, France
[2] Developmental Biology Unit, European Molecular Biology Laboratory, Meyerhofstrasse 1, 69117 Heidelberg, Germany
[3] UMC Utrecht, Department of Cell Biology and the Institute of Biomembrane, AZU, Rm G02.525, Heidelberglaan 100, 3584 CX Utrecht, The Netherlands
*Correspondence: ephrussi@embl.de (A.E.), c.rabouille@umcutrecht.nl (C.R.)
DOI 10.1016/j.devcel.2007.03.002

SUMMARY

In *Drosophila*, localized activity of *oskar* at the posterior pole of the oocyte induces germline and abdomen formation in the embryo. Oskar has two isoforms, a short isoform encoding the patterning determinant and a long isoform of unknown function. Here, we show by immuno-electron microscopy that the two Oskar isoforms have different subcellular localizations in the oocyte: Short Oskar mainly localizes to polar granules, and Long Oskar is specifically associated with endocytic membranes along the posterior cortex. Our cell biological and genetic analyses reveal that Oskar stimulates endocytosis, and that its two isoforms are required to regulate this process. Furthermore, we describe long F-actin projections at the oocyte posterior pole that are induced by and intermingled with Oskar protein. We propose that Oskar maintains its localization at the posterior pole through dual functions in regulating endocytosis and F-actin dynamics.

INTRODUCTION

Oskar is a determinant of embryonic polarity whose expression during *Drosophila* oogenesis is spatially restricted to the posterior pole of the oocyte through complementary processes: asymmetric localization of *oskar* mRNA, localization-dependent translation, and maintenance of Oskar protein at the posterior pole (Lehmann and Nüsslein-Volhard, 1986; Kim-Ha et al., 1991, 1995; Ephrussi et al., 1991; Rongo et al., 1995; Markussen et al., 1995; Vanzo and Ephrussi, 2002). Regulated expression of *oskar* at the posterior pole is critical, as Oskar induces the formation of the pole plasm, a specialized cytoplasm containing the abdominal and germline determinants of the fly (Ephrussi and Lehmann, 1992). Pioneer ultrastructural investigations by electron microscopy revealed that the pole plasm contains characteristic electron-dense ribonucleo-protein organelles, called polar granules (Mahowald, 1962). Subsequently, transplantation experiments in the early embryo showed that the presence of polar granules correlates with germline-determining activity (Illmensee and Mahowald, 1974). Polar granules are absent from the posterior pole of embryos produced by *oskar* mutant females (Lehmann and Nüsslein-Volhard, 1986), revealing a critical function of *oskar* in their biogenesis. Consistent with this function are the onset of *oskar* mRNA translation at the stages (8 onward) and site of polar granule formation during midoogenesis (Kim-Ha et al., 1995; Rongo et al., 1995; Markussen et al., 1995) and the presence of Oskar, detected by electron microscopy, in polar granules in the early embryo (Breitwieser et al., 1996).

How Oskar protein nucleates polar granules during oogenesis is largely unknown at the molecular level, except that it is thought to involve the recruitment of other maternally encoded pole plasm components, such as the DEAD-box RNA helicase Vasa (Breitwieser et al., 1996, and references therein). *oskar* encodes two protein isoforms, Long and Short Oskar, translated from in-phase alternative initiation codons in *oskar* mRNA. Only Short Oskar directs the formation of the pole plasm and its polar granules, as shown by its unique ability to specify pole cells in the early embryo (Markussen et al., 1995; Breitwieser et al., 1996). In contrast, Long Oskar is necessary for the maintenance of *oskar* mRNA after its localization at the posterior pole of the oocyte and for the efficient anchoring of Short Oskar at the oocyte cortex (Markussen et al., 1995; Rongo et al., 1995; Vanzo and Ephrussi, 2002). In the absence of Long Oskar, both *oskar* mRNA and Short Oskar largely delocalize from the posterior of late-stage oocytes, in discrete particles in which Vasa colocalizes, leading to patterning and germline-formation defects in the progeny (Vanzo and Ephrussi, 2002). Thus, Long Oskar-mediated maintenance of the pole plasm-inducing function of Short Oskar is critical during oogenesis, emphasizing the importance of understanding the molecular mechanisms by which Short and Long Oskar exert their respective functions.

In this study, we have used immuno-electron microscopy to localize the two Oskar isoforms at an ultrastructural level in stage-10 oocytes, when polar granules form and Oskar maintenance is ongoing. Our analysis reveals that the two isoforms exhibit distinct localizations at the posterior pole—Short Oskar localizing mainly on polar

granules and Long Oskar on endocytic membranes. Furthermore, we show that both endocytosis and the structure of the F-actin cytoskeleton are asymmetric at the cortex of wild-type oocytes, and that Oskar is essential for these asymmetries. We hypothesize that regulation of endocytosis and F-actin by Oskar, in turn, reinforces Oskar maintenance at the posterior pole of the oocyte.

RESULTS

The Two Oskar Isoforms Exhibit Distinct Subcellular Localizations

To investigate the subcellular distribution of the two Oskar isoforms during oogenesis, we first performed immunoelectron microscopy (IEM) on cryo-sections of stage-9 and -10 wild-type oocytes, using an anti-Oskar antibody that recognizes the region common to the two isoforms (Figure 1A). The immuno-gold labeling was highly enriched in the most posterior region of the oocyte, in electron-dense, non-membrane-bound structures similar to polar granules (Mahowald, 1962). Double labeling with antibodies directed against the polar granule components Oskar and Vasa (Hay et al., 1988; Breitwieser et al., 1996) (Figure 1B) revealed colocalization of the proteins in these structures, unambiguously identifying them as polar granules. About 50 polar granules, each with a diameter of 190 ± 90 nm, were present per ultrathin section at the oocyte posterior pole, which we defined as the space contained within the first 1–1.5 μm beneath the posterior plasma membrane and reaching about 15–20 μm laterally from the most posterior point. Quantification of the distribution of gold particles revealed that, within this space and at stages 9/10, only 60% of Oskar is localized on polar granules (see Table S1 in the Supplemental Data available with this article online). Another 20% of Oskar is detected in the posterior ooplasm, seemingly not associated with any structure. Most striking, the remaining 20% is closely associated with the membrane of vesicles and tubules that are mainly unlabeled by Vasa (arrowheads, Figures 1A and 1B). Unlike polar granules, which are only present at the posterior pole, Oskar is also detected on endocytic membrane along the lateral subcortex of the oocyte, albeit at a much weaker level (Figure S1B). To confirm the specificity of our immunodetection, we probed sections of oocytes in which no Oskar protein is produced ($osk^{54}/Df(3R)p^{XT103}$ and osk^{54}/osk^{84}) with the same anti-Oskar antibody. On these sections, only scarce gold labeling was observed in the whole ooplasm, with no labeling of cortical membranes either posteriorly or laterally (Figure S1A). Thus, in addition to its concentration on polar granules from midoogenesis onward, a substantial proportion of Oskar is distributed in the ooplasm and on membrane structures at the oocyte posterior pole.

Short Oskar, the pole plasm-inducing isoform of Oskar, interacts with and recruits Vasa (Markussen et al., 1995; Breitwieser et al., 1996). Therefore, the selective localization of Vasa to polar granules and its absence from

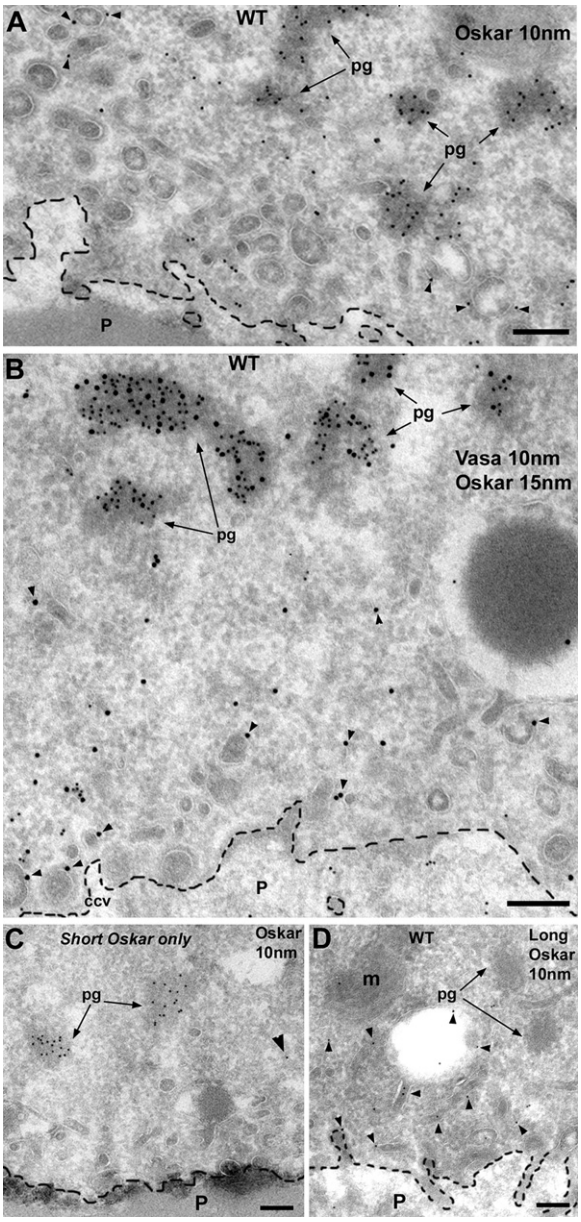

Figure 1. Short Oskar and Long Oskar Localize to Polar Granules and Membrane, Respectively

(A and B) Immunolocalization of Oskar with a rabbit anti-Oskar serum recognizing (A) the two Oskar isoforms together with (B) Vasa on ultrathin cryosections of stage-10 wild-type (WT) oocytes.

(C) Immunolocalization of Short Oskar on ultrathin cryosections of stage-9 *oskar* protein null oocytes ($osk^{54}/Df(3R)p^{XT103}$) expressing the transgene P(*oskM1R*) encoding for Short Oskar and labeled with the rabbit anti-Oskar serum (see [A]).

(D) Immunolocalization of Long Oskar on ultrathin cryosections of stage-10 wild-type oocytes, with a polyclonal serum raised against the amino-terminal extension (M1M2) of Long Oskar. Arrowheads points at the labeling for (A and B) Oskar and (D) Long Oskar associated with membrane. The plasma membrane is marked by a dashed line. P, posterior of the oocyte; pg: polar granules; m, mitochondria. The scale bars are 200 nm.

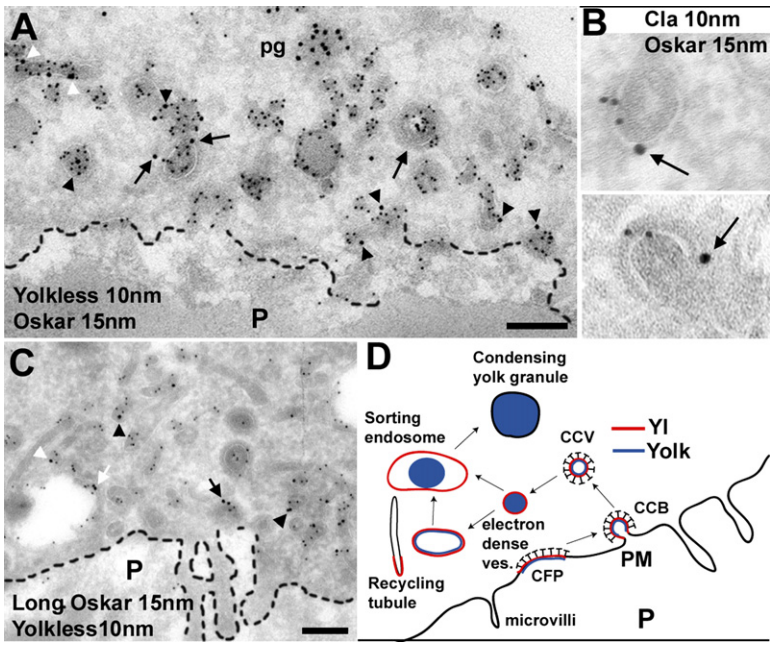

Figure 2. Localization of Long Oskar on the Endocytic Membrane

(A–C) Immunolocalization of Oskar (15 nm) together with (A) Yolkless (10 nm) and (B) clathrin heavy chain (Cla, 10 nm), and of (C) Long Oskar and Yolkless (10 nm) on ultrathin cryosections of stage-10 wild-type oocytes. Black arrows indicate clathrin-coated structures (flat pits, buds, and vesicles, see [D]) that are positive for Oskar and Long Oskar. Black arrowheads highlight Oskar-positive, uncoated, electron-dense vesicles; white arrows and arrowheads, Oskar-positive sorting endosomes and tubules, respectively.

(D) Diagram showing all of the different endocytic structures of a vitellogenic oocyte. These are all positive for Oskar and Long Oskar (see Table S1). Membrane compartments labeled with Yolkless (Yl, red) and yolk proteins (blue) are depicted. PM, plasma membrane; CFP, clathrin-coated, flat pits; CCB, clathrin-coated buds; CCV, clathrin-coated vesicles; P, posterior of the oocyte. The scale bars are 200 nm.

Oskar-positive membranes (Figure 1B) suggested that the two subcellular distributions of Oskar that we observed might reflect a differential distribution of the two isoforms. To test this hypothesis, we investigated the distribution of Short Oskar and Long Oskar separately. We first examined the distribution of Short Oskar in transgenic oocytes exclusively expressing this isoform (Vanzo and Ephrussi, 2002), as the entire Short Oskar peptide is included within Long Oskar, rendering the selective immunodetection of Short Oskar in wild-type oocytes impossible. We focused our study on stage-9 oocytes, in which Short Oskar localization is apparently unaffected by the absence of Long Oskar (Vanzo and Ephrussi, 2002). At this stage, the transgenic oocytes display largely normal polar granule formation, as judged by their number: 13.7 ± 1.8 and 16.9 ± 3.3 polar granules/10 μm posterior plasma membrane in *oskar* mutant oocytes expressing Short Oskar alone and wild-type oocytes, respectively. The vast majority (87%) of Short Oskar is detected on the polar granules (Figure 1C; Table S1). The remaining labeling is detected in the cytoplasm and, at a very low level, on membranes (data not shown). The distribution of Short Oskar in these oocytes is very similar to that of Vasa in wild-type oocytes (Figure 1B), consistent with the role of Short Oskar in Vasa recruitment.

We next examined the distribution of Long Oskar, which at stage 10 is required for the maintenance of Short Oskar at the posterior cortex (Vanzo and Ephrussi, 2002). To selectively detect Long Oskar in wild-type oocytes, we generated an antibody specific to the amino-terminal extension (M1M2 region) (Gunkel et al., 1998), which is absent from Short Oskar (Markussen et al., 1995). Specificity of the antibody was confirmed by its ability to selectively detect Long Oskar (Figure S2A). When used in IEM, this antibody revealed that Long Oskar is primarily associated with membrane structures (75%) and is practically absent from polar granules in stage-9 and -10 wild-type oocytes (Figure 1D; Table S1). Residual labeling is present throughout the posterior cytoplasm.

Taken together, these data show that the two Oskar isoforms localize to distinct subcellular structures at the posterior pole of the oocyte during stages of polar granule formation and maintenance. The main pool of Short Oskar resides in polar granules, whereas Long Oskar predominantly associates with membrane structures at the posterior pole.

Oskar Associates with Endocytic Membranes at the Oocyte Cortex

To gain insight into the significance of the membrane localization of Long Oskar, we next characterized the membranes with which the protein is associated. In the *Drosophila* oocyte, the endosomal compartment has been described morphologically as restricted to within 1 μm beneath the plasma membrane (Tsuruhara et al., 1990, and references therein), which coincides with the location of Oskar-positive membranes. During the vitellogenic stages (midoogenesis onward), this compartment is engaged in receptor-mediated endocytosis of large amounts of vitellogenins (yolk proteins, YPs) that are stored in the oocyte in yolk granules (DiMario and Mahowald, 1987; Tsuruhara et al., 1990). The vitellogenin receptor, Yolkless, which, after clathrin-mediated internalization, returns to the oocyte plasma membrane through recycling tubular structures, marks all endocytic structures except the yolk granules (Figure 2D) (DiMario and Mahowald, 1987; Schonbaum et al., 2000). Analysis of the relative distributions of Oskar and Yolkless in wild-type oocytes by IEM revealed that all of the membrane structures with which Oskar associates are also positively

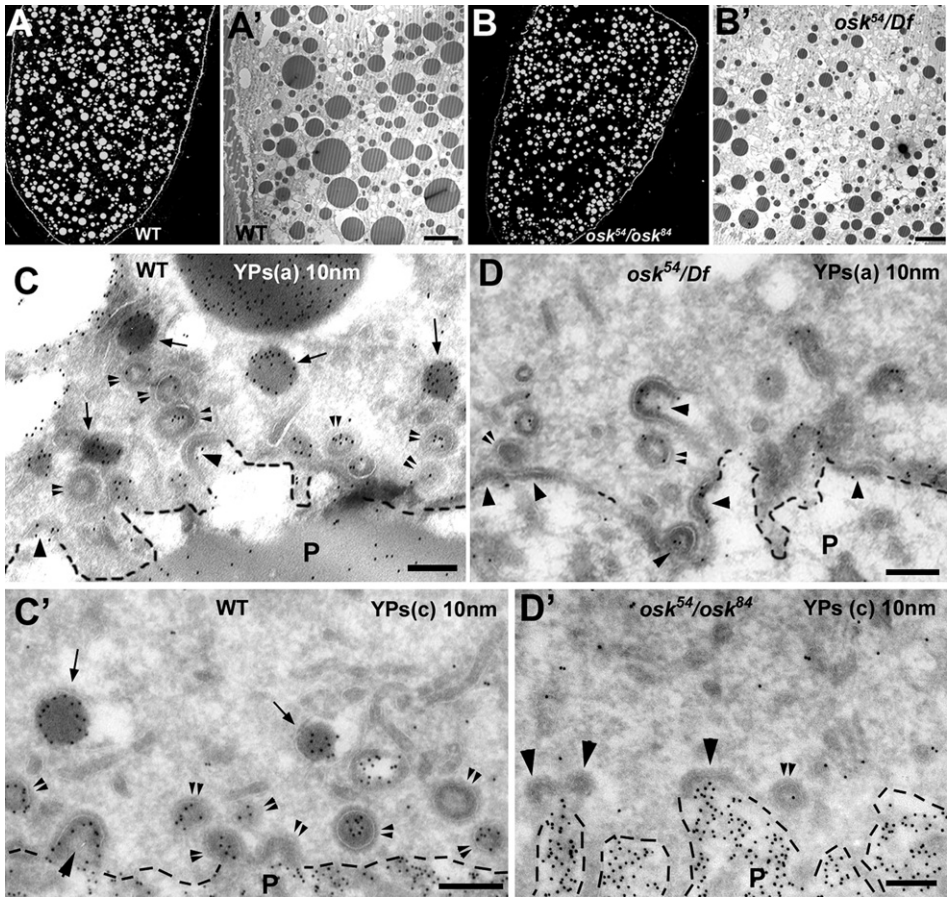

Figure 3. YP Uptake Is Impaired in the Absence of Oskar

(A–B′) Visualization of the Yolk granule content in (A and A′) wild-type and (B and B′) *oskar* protein null stage-10 oocytes by (A and B) immunofluorescence microscopy of YPs on semi-thick cryosections and on (A′ and B′) low-magnification electron micrographs of ultrathin cryosections. The cortical labeling in (A) and (B) corresponds to the perivitelline space in (A) and (B) (follicle cell-oocyte interface). The posterior pole is located at the bottom of the figure. The scale bars are 5 μm.

(C–D′) Immunolocalization of YPs at the posterior pole of (C and C′) stage-10 wild-type and (D and D′) *oskar* protein null oocytes. Two independent anti-YP sera (noted a in [C] and [D] and c in [C′] and [D′]) were used. Note the reduced labeling of YPs in the endocytic compartment of the mutant compared to wild-type oocytes (quantified in Table 1). Arrowheads and double arrowheads point to the clathrin-coated vesicles and clathrin-coated buds/flat pits, respectively. Arrows point to uncoated, electron-dense vesicles. P, posterior. The scale bars are 200 nm.

labeled for Yolkless (Figure 2A). This result indicates that Oskar localizes on endocytic structures; these include flat, clathrin-coated pits of the plasma membrane (CFP), buds (CCB), and vesicles (CCV), as revealed by immuno-gold detection of clathrin heavy chain (Figure 2B) and α-adaptin (data not shown). Oskar is also present on uncoated, electron-dense, 100–150 nm vesicles, sorting endosomes, and recycling tubules. The same Yolkless-positive structures are labeled with the antibody that selectively detects Long Oskar (Figure 2C), confirming the specific association of this isoform with the endocytic compartment. The relative distribution of Oskar on the various endocytic structures was more precisely quantified (Table S1) and is essentially proportional to the relative abundance of those membranes at the posterior cortex (data not shown). Thus, Oskar, and specifically Long Oskar, appears to associate equally with all categories of membrane of the endocytic compartment.

Oskar Upregulates Endocytosis

Our finding that Oskar localizes on endocytic membranes was unexpected and prompted us to investigate whether the protein might play a role in endocytosis. From midoogenesis onward, endocytosis in the oocyte is mostly dedicated to the uptake of YPs that are stored in yolk granules in the growing oocyte (DiMario and Mahowald, 1987). We therefore compared the yolk content of stage-10 wild-type and *oskar* protein null oocytes, visualizing the yolk granules both directly, by electron microscopy of ultrathin cryosections, and indirectly, by confocal immunofluorescence with an anti-YP antiserum. This analysis revealed that yolk granules occupy 2-fold less volume in *oskar* null than in wild-type oocytes (Figures 3A–3B′; Table 1, column 1). This reduction suggested that YP accumulation is impaired in *oskar* mutant oocytes.

To examine whether the reduction in yolk granule content could reflect a defect in endocytosis of YPs in *oskar*

Table 1. Morphometric Analysis of Endocytic Defects at the Posterior Pole of Stage-10 *oskar* Protein Null Oocytes

	Posterior Pole						Lateral Cortex	
	1	2	3	4			5	6
Genotype	Yolk Content[a]	Total Surface of Endocytic Structures (μm^2/10 μm PM)	Immunolabeling of YPs in Endocytic Structures (Gold/10 μm PM)	Percentage of Clathrin-Coated Structures CCV[b]	CCB[b]	CFP[b]	Total Surface of Endocytic Structures (μm^2/10 μm PM)	Immunolabeling of YPs in Endocytic Structures (Gold/10 μm PM)
WT	35% ± 2%	0.63 ± 0.05	137 ± 42[c], 190 ± 50[d]	41.6 ± 2	43.2 ± 3	15.2 ± 2	0.40 ± 0.07	76 ± 25[c], 90 ± 18[d]
osk^{54}/*osk*^{84}	19% ± 4%	0.34 ± 0.08	61 ± 28[c]	30.4 ± 3	19.3 ± 2	50.3 ± 3	0.29 ± 0.1	57 ± 10[c]
osk^{54}/*Df(3X)p*^{XT103}	18% ± 3%	0.32 ± 0.08	26 ± 12[d]	nd	nd	nd	0.29 ± 0.1	27 ± 13[d]

[a] Estimated by electron microscopy or/and immunofluorescence (see Experimental Procedures).
[b] CCV, clathrin-coated vesicles; CCB, clathrin-coated buds; CFP; clathrin-coated, flat pits.
[c,d] Quantifications have been performed by immunodetection on ultrathin cryosections by using two independent anti-YPs sera described by Warren and Mahowald (1979) and Trougakos et al. (2001) for sera a and b, respectively.

mutant oocytes, we analyzed the uptake of vitellogenins at the oocyte plasma membrane by IEM. We first concentrated our analysis on the posterior of the oocyte, where Oskar protein is translated and anchored. In wild-type oocytes, vitellogenins are distributed on clathrin-coated structures (double arrowheads in Figures 3C and 3C′), which mediate Yolkless internalization (Schonbaum et al., 2000), on uncoated, electron-dense 100–150 nm vesicles (arrows in Figures 3C and 3C′), on sorting endosomes (Figure S3), and on enlarged condensing yolk spheres at different stages of maturation. In contrast, in *oskar* mutant oocytes, YP labeling is mainly concentrated along the plasma membrane on expanded flat, clathrin-coated pits (noted CFP in Figure 2D, single arrowheads in Figures 3D and 3D′), where Yolkless also concentrates (Figure S3). Strikingly, clathrin-coated vesicles, when observed in *oskar* mutant oocytes, appear depleted of YPs, compared to those observed in wild-type oocytes (compare Figures 3C–3D′). Intermediate/late endocytic structures, such as electron-dense vesicles, sorting endosomes, and condensing yolk granules, are less numerous in *oskar* mutant, compared to wild-type, oocytes (compare arrows in Figures 3C–3D′).

To further characterize this mutant phenotype, we quantified both the overall size and the degree of YP labeling of early and intermediate endocytic structures, comprising coated profiles, uncoated vesicular/tubular profiles, and electron-dense vesicles up to 1 μm beneath the plasma membrane (see Experimental Procedures). This analysis revealed that, in *osk*^{54}/*osk*^{84} oocytes, both the size of the endocytic compartment (Table 1, column 2) and its overall YP labeling (Table 1, column 3) are reduced 2-fold, compared to wild-type oocytes. To validate this finding, we repeated the analysis by using an independent anti-YP serum and a different combination of *oskar* protein null alleles (*osk*^{54}/*Df(3R)p*^{XT103}). Quantification again revealed an ~ 2-fold reduction in the size of endocytic structures in *oskar* mutant, compared to wild-type, oocytes (Table 1, column 2). The reduction in YP labeling was also confirmed, and it was, in fact, more pronounced in these conditions (7-fold, see Table 1, column 3). Thus, Oskar is required for wild-type levels of endocytosis at the posterior pole.

Mutations impeding the expression of Yolkless or its localization to the endocytic compartment of the oocyte have been shown to alter both the uptake of YPs and the general morphology of the endocytic compartment in the oocyte (DiMario and Mahowald, 1987; Sommer et al., 2005). Although we observed similar defects in *oskar* oocytes (see above), Yolkless appears to be properly distributed on endocytic membranes in this mutant (Figure S3). Thus, Yolkless trafficking per se does not seem to be affected in the mutant.

Oskar Stimulates Primary Steps of Clathrin-Mediated Endocytosis

Whereas endocytosed structures are less abundant in *oskar* protein null oocytes than in wild-type oocytes, the flat, clathrin-coated pits are more prominent (see above). We therefore focused our analysis on and quantified the clathrin-coated structures near the plasma membrane. In wild-type oocytes, the major clathrin-coated profiles are coated buds and vesicles (Table 1, column 4). In contrast, flat, clathrin-coated pits are scarce. Although the total number of clathrin-coated structures per unit length of plasma membrane does not differ significantly in *oskar* null and wild-type oocytes, the relative proportion of the different types of structures does. Indeed, flat, clathrin-coated pits are the most prominent coated structures in the *oskar* mutant oocytes, where their percentage is 3-fold greater than in wild-type. This increase in flat, clathrin-coated pit number is paralleled by an increase in their size. Conversely, the number of coated buds and vesicles is reduced in *oskar* mutant oocytes. This analysis shows that very early steps of clathrin-mediated endocytosis are slowed down in *oskar* protein null oocytes, suggesting that Oskar might stimulate the dynamics of this process. This finding could account for the partial clearance of intermediate/late endocytic structures, in particular the electron-dense vesicles that we observed in the mutant (see above). Taken together, these results suggest that Oskar upregulates endocytosis.

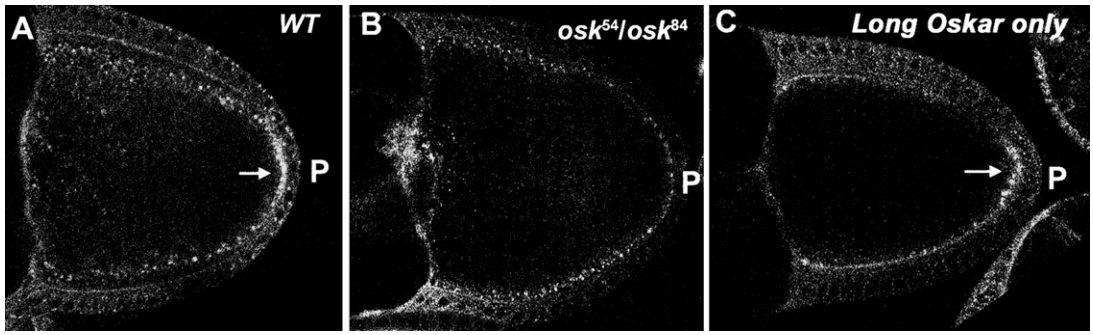

Figure 4. Oskar Promotes Asymmetric Levels of Endocytosis in the Oocyte

(A–C) FM4-64 uptake in living (A) wild-type oocyte, (B) *oskar* protein null oocytes (osk^{54}/osk^{84}), and (C) *oskar* protein null oocytes expressing Long Oskar from a transgene (P[*oskM139L*]; osk^{54}/osk^{84}) at stage 10. The strong accumulation of FM4-64 at the posterior pole is indicated by a white arrow.

Oskar Maintains Asymmetric Levels of Endocytosis over the Oocyte Cortex

Endocytosis of YPs occurs all over the oocyte cortex during the vitellogenic stages. If, as our above data suggest, Oskar stimulates endocytosis, one would predict endocytosis to be greater at the posterior pole, where Oskar is concentrated, than along the lateral cortex. We indeed found that, in wild-type oocytes at stage 10, both the surface area and the labeling of the endocytic compartment are higher at the posterior than at the lateral cortex (Table 1, compare column 2 with column 5 and column 3 with column 6). Thus, endocytic activity is asymmetric around the oocyte cortex.

To determine if Oskar is required for this observed asymmetry, we repeated this analysis in *oskar* mutants. This analysis revealed that the lateral and posterior regions are essentially indistinguishable in *oskar* oocytes, both in terms of the abundance and the degree of labeling of endocytic structures (Table 1, compare column 2 with column 5 and column 3 with column 6). We therefore conclude that Oskar is required to establish or maintain asymmetric levels of endocytosis along the oocyte cortex.

We further assessed the endocytic process in live oocytes by using a functional assay based on the uptake of the membrane-selective dye FM4-64 (Sommer et al., 2005). This fluorescent dye can be used to image the dynamics of endocytosis, including the early steps after plasma membrane invagination. To visualize the endocytic compartments, wild-type oocytes were briefly incubated with the dye and were then extensively washed to minimize plasma membrane labeling (see Experimental Procedures). Under these conditions, the fluorescence is associated with endocytic structures, which are more numerous and intensely labeled at the posterior pole than laterally (Figure 4A), reflecting enhanced endocytosis at the posterior in wild-type oocytes. In contrast, in *oskar* protein null oocytes, posterior and lateral endocytic cortex were uniformly stained (Figure 4B). This functional endocytic assay strongly supports our previous finding that Oskar upregulates endocytosis at the posterior pole of the oocyte.

Long and Short Oskar Cooperate in Regulating Clathrin-Mediated Endocytosis

As it localizes mainly on endocytic membranes, Long Oskar might be involved in the upregulation of endocytosis at the posterior pole. However, the specific function of Long Oskar in this process cannot be assessed by loss-of-function experiments, as Short Oskar accumulation and anchoring are also impaired in the absence of Long Oskar (Vanzo and Ephrussi, 2002). We therefore examined whether sole expression of Long Oskar could stimulate endocytosis in *oskar* null oocytes. To this aim, we made use of a transgenic construct expressing wild-type levels of Long Oskar at the posterior pole (Vanzo and Ephrussi, 2002). At stage 10, *oskar* mutant oocytes expressing this transgene were found to contain amounts of yolk granules similar to those in wild-type (Figure 5A). Thus, on its own, Long Oskar can promote vitellogenin uptake to wild-type levels. The oocytes also displayed brighter FM4-64-associated fluorescence in endocytic structures at the posterior pole, revealing that Long Oskar also enhances endocytosis at this position (Figure 4C).

Upon closer examination of endocytosis by IEM, striking differences in the morphology of the endocytic compartment were observed in transgenic Long Oskar-expressing oocytes, compared to wild-type oocytes. Clathrin-coated structures (CCP and CCV) were reduced in the transgenic oocytes and, when present, were largely devoid of vitellogenins (compare Figures 3C and 3C′ and Figures 5B–5C″, double arrowheads). Uncoated, electron-dense, 100–150 nm vesicles, which are intermediate structures in clathrin-mediated endocytosis, are also scarcely seen in the posterior ooplasm of those transgenic oocytes. As clathrin-coated structures underlie receptor-mediated endocytosis (DiMario and Mahowald, 1987), we conclude that, in oocytes expressing Long Oskar alone, vitellogenins are internalized via an alternative type of endocytosis.

Remarkably, in this background, we observed two prominent types of profiles heavily labeled by anti-YPs. The first type consists of long cytoplasmic protrusions of the plasma membrane (Figure 5B) that are sometimes

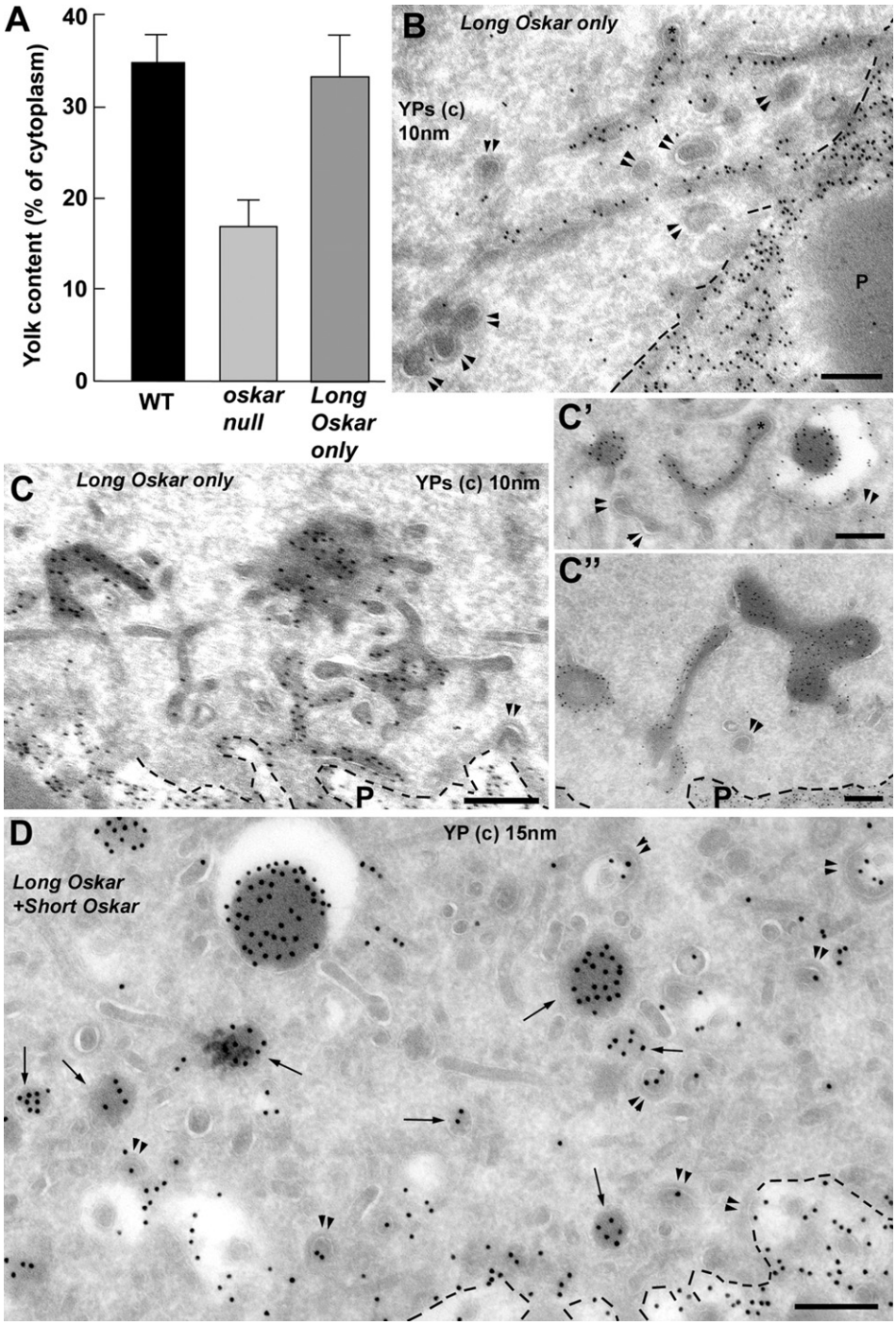

Figure 5. Long and Short Oskar Cooperate in the Regulation of Clathrin-Mediated Endocytosis

(A) Quantification of the yolk granule content in wild-type oocytes (WT), *oskar* protein null oocytes (osk^{54}/osk^{84}), and in *oskar* protein null oocytes expressing Long Oskar from a transgene (P[*oskM139L*]; osk^{54}/osk^{84}) at stage 10, on low-magnification electron micrographs of ultrathin cryosections (as presented in Figures 3A′ and 3B′).

(B–D) Immunolocalization of YPs (with the antisera c) in stage-10 *oskar* protein null oocytes (osk^{54}/osk^{84}) expressing either (B–C″) Long Oskar alone, from the transgene P(*oskM139L*), or (D) both Oskar isoforms, from the transgenes P(*oskM1R*) and P(*oskM139L*). Double arrowheads point to clathrin-coated pits and vesicles; Arrows to uncoated, electron-dense vesicles. P, posterior. The scale bars are 200 nm.

clathrin coated at their tip or laterally. As mentioned above, those coated structures are mainly devoid of YPs. The second type consists of more electron-dense, pleiomorphic tubular/vacuolar structures, located near, but not continuous with, the plasma membrane. These structures are frequently located near condensing yolk

structures, suggesting that they might directly deliver their YP content to the large, maturing yolk granules (Figure 5C′), or that they might themselves mature into yolk granules (Figures 5C and 5C″). Both types of profiles were found to span several sections (data not shown), indicating that, rather than being tubes, they represent large invaginations of plasma membrane. This suggests that tubular/vacuolar structures present inside the ooplasm could be formed by detachment and maturation of the plasma membrane protrusions described above. Alternatively, they could correspond to two independent types of membrane invaginations. Taken together, these data show that Long Oskar stimulates yolk endocytosis through an alternative, yet efficient, non-clathrin-mediated pathway involving large, sheet-like involutions of plasma membrane.

To determine whether this pathway of endocytosis is induced in response to nonphysiological conditions associated with sole expression of Long Oskar, we re-expressed Short Oskar in those oocytes from a second transgene. There, the morphology of the endocytic compartment was indistinguishable from that of wild-type oocytes. In particular, clathrin-coated structures and intermediate electron-dense vesicles, heavily stained by vitellogenins, were restored (Figure 5D; compare to Figures 3C and 3C′). Thus, although Long Oskar potently stimulates endocytosis on its own, both isoforms are required to promote the wild-type clathrin-mediated pathway of endocytosis.

Oskar Regulates Cortical Actin Organization in the Oocyte

A functional link has emerged between endocytosis and the actin cytoskeleton at the cortex of many cells (reviewed in Engqvist-Goldstein and Drubin, 2003). Actin polymerization is thought to drive membrane invagination, vesicle fission, and the movement of vesicles. Thus, given the slow-down of clathrin-coated vesicle formation in *oskar* null oocytes, we wondered whether the cortical F-actin cytoskeleton might also be affected.

To test this idea, we compared the fine organization of the F-actin cytoskeleton at the posterior pole of wild-type and *oskar* null oocytes, by using confocal microscopy at a high magnification (see Experimental Procedures). In the majority of wild-type oocytes (88%, n = 18), we reproducibly observed discrete, very thin, long (average 2.5 μm) projections of F-actin into the ooplasm (Figures 6A and 6A′). These projections appear to emanate from the packed actin bundles overlying the posterior cortex of the oocyte and are rarely observed along the lateral cortex (Figure S4). Remarkably, when Oskar is immunodetected with F-actin, dot-like structures marked by Oskar, which probably correspond to polar granules (or clusters of polar granules), are observed closely apposed to, or overlapping with, the dense actin projections (Figure 6A′, inset). In contrast, only a minority (10%, n = 19) of *oskar* null oocytes exhibit such actin projections at the posterior pole. Indeed, the majority of these oocytes shows a significant reduction in the density of these projections, as well as in their length (average of 1.2 μm; Figures 6B and 6B′). The expression of Long Oskar in *oskar* null oocytes does not lead to the formation of such F-actin projections (Figure 6C). In contrast, coexpression of Long Oskar and Short Oskar in *oskar* null oocytes promotes their formation to a wild-type level (Figure 6D). Taken together, these results reveal that the joint activities of the two Oskar isoforms, either directly or via the polar granules they induce, influence the specific organization of the cortical actin cytoskeleton at the posterior of the oocyte.

DISCUSSION

Our investigation of the subcellular localization of Oskar in the *Drosophila* oocyte has uncovered an unanticipated function of Oskar in endocytosis. Using IEM, we found that Short and Long Oskar are mostly concentrated on distinct cellular structures in the oocyte—the polar granules and the endocytic compartment, respectively. Using stereological methods and functional assays, we have shown that endocytosis levels are asymmetric around the cortex of wild-type oocytes, and that high levels of endocytosis at the posterior pole require Oskar expression. In addition, *oskar* mutant oocytes exhibit both a reduced endocytosis of yolk proteins and a reduction in endocytic structures at the posterior plasma membrane. Finally, we have identified a function of Oskar in the asymmetric organization of the F-actin cytoskeleton in the oocyte. Our data strongly suggest that both isoforms are potent regulators of endocytosis and F-actin dynamics.

Long Oskar and Short Oskar Localize Differentially at the Oocyte Posterior Pole

The localization of the two Oskar isoforms to distinct subcellular structures during oogenesis may account for the previous unexplained observation of their distinct segregation during early embryogenesis, when the primordial germ cells form (Markussen et al., 1995). Indeed, during these stages, Short Oskar accumulates in the pole cells, the future germ cells. We have found that, during oogenesis, Short Oskar mainly concentrates in the polar granules. This localization is consistent with the previously reported function of this isoform in the establishment of the germ cell lineage in the embryo (Markussen et al., 1995), a process thought to be instructed by polar granules. In contrast, Long Oskar is selectively excluded from pole cells in the early embryo and shows a specific affinity for membranous structures during oogenesis. Thus, the differential localization of the two Oskar isoforms that originates in oogenesis could persist over the lifetime of the two proteins and specify distinct destinies—Short Oskar being incorporated in the germ cells, and Long Oskar not.

Distinct localizations of the two Oskar isoforms could be due to the amino-terminal extension of Long Oskar (M1M2). However, this extension is unlikely sufficient to explain the specific association of Long Oskar with endocytic membranes, as Short Oskar can also associate with these, at a very low level. This extension might either increase the membrane affinity of Long Oskar and/or

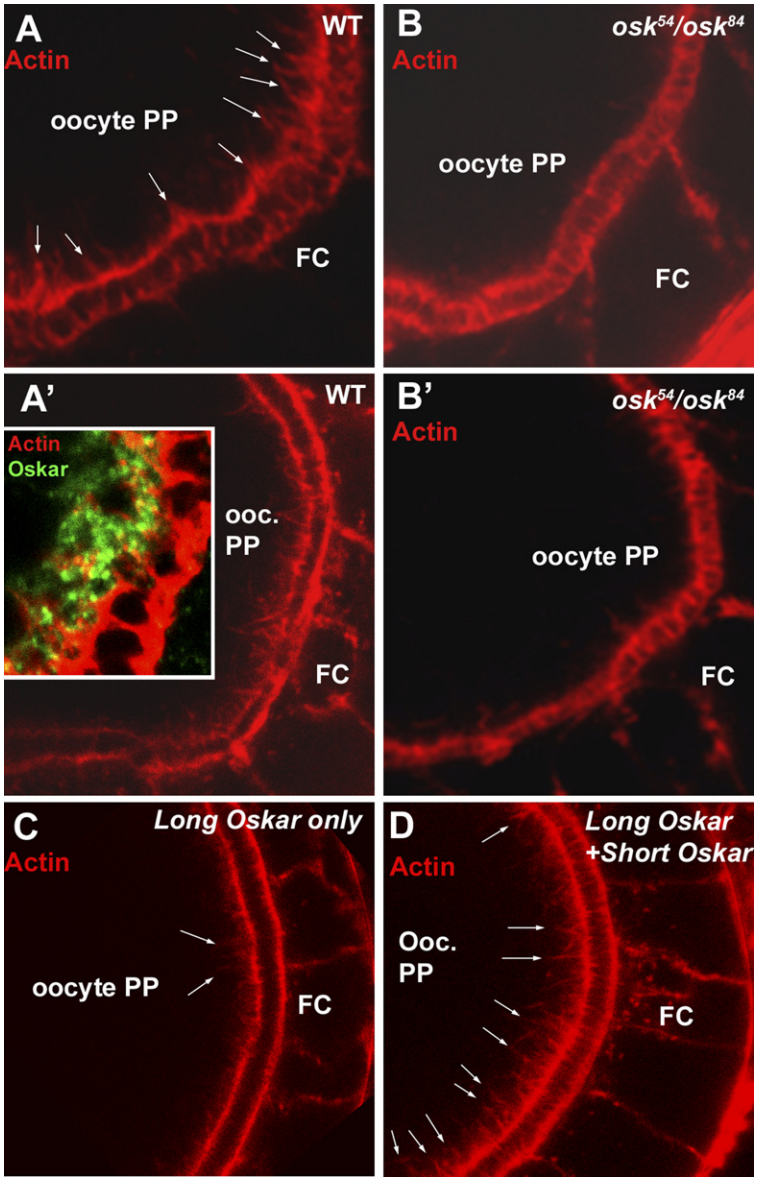

Figure 6. Cortical Actin Organization Is Modified in *oskar* Protein Null Oocytes

(A–D) Confocal analysis of the actin cytoskeleton at the posterior pole of stage-10 oocytes from (A and A′) wild-type, (B and B′) *oskar* protein null (osk^{54}/osk^{84}), (C) *oskar* protein null in which Long Oskar alone is expressed from the transgene P(*oskM139L*), and (D) *oskar* protein null in which both Short and Long Oskar are expressed from the transgenes P(*oskM1R*) and P(*oskM139L*), respectively. F-actin is labeled with phalloidin (red), and Oskar protein (green, inset in [A′]) is detected by immunofluorescence with a rabbit antibody to Oskar. White arrows indicate the long F-actin projections, which are ~2.5 μm in length. PP, posterior pole; FC, follicle cells.

provide additional elements for efficient targeting/recruitment. It is noteworthy that Long Oskar is not an integral membrane protein. Neither a signal peptide, required for ER targeting, nor a significant hydrophobic stretch, required for membrane insertion, are apparent in its primary sequence. It is therefore presumably a peripheral protein recruited from the ooplasm to the cytosolic face of the endocytic membrane.

The absence of Long Oskar from polar granules is surprising for two reasons. First, Long Oskar is required for the maintenance of Short Oskar at the posterior pole of the oocyte (Vanzo and Ephrussi, 2002). This implies that the maintenance function of Long Oskar must operate in an indirect way (see below). Second, in addition to its specific amino-terminal extension, Long Oskar contains the entire Short Oskar peptide (Markussen et al., 1995). This suggests that the N-terminal extension inhibits polar granule association of Long Oskar, in addition to promoting its association with membranes (see above). As the polar granule component Vasa is not found on Long Oskar-positive membranes, this extension might also prevent Long Oskar from recruiting/assembling polar granule components, explaining its failure to specify the germline and the abdomen (Markussen et al., 1995; Breitwieser et al., 1996).

How Does Oskar Regulate Clathrin-Mediated Endocytosis in the *Drosophila* Oocyte?

We have shown that, in *oskar* null oocytes, clathrin-mediated endocytosis is affected, both in its efficiency and its asymmetry. The aberrant prominence of flat, clathrin-coated areas of plasma membrane, instead of coated pits and vesicles, in those oocytes suggests impairment of endocytosis at an early stage, possibly in

the initial invagination of the plasma membrane (Kirchhausen, 2002). This reveals that Oskar is a novel regulator of endocytosis.

The finding that sole expression of Long Oskar in *oskar* null oocytes triggers the formation of long and dense membrane sheet invaginations whose formation is abrogated upon coexpression of Short Oskar from a second transgene provides plausible explanations for the function of Oskar isoforms. Long Oskar could trigger an early step in the formation of clathrin-mediated membrane invaginations, which, in the absence of Short Oskar, fail to pinch off as coated vesicles and, instead, become protrusions, as observed in the dynamin mutant *shibire* (shi^{ts}) at the restrictive temperature (Kessell et al., 1989; Tsuruhara et al., 1990). Very reminiscent of abortive coated extensions also described in *shibire* oocytes, we observed numerous clathrin-coated buds forming at the tip and sides of the large plasma membrane invaginations in oocytes expressing only Long Oskar. In these oocytes, the invaginations may eventually detach and mature into yolk granules. The fact that these invaginations are no longer observed when Short Oskar is present suggests that Short Oskar could have a specific function in the subcellular localization and/or activation of dynamin at the posterior pole. The second, not exclusive, possibility is that Long Oskar activates membrane invagination through a clathrin-independent mechanism of endocytosis that Short Oskar antagonizes/overcomes to promote classical clathrin-mediated endocytosis. Clathrin-independent endocytosis has long been proposed and has recently been shown to involve tubular pleiomorphic structures very similar to those we observed in the ooplasm of oocytes expressing Long Oskar only (Kirkham et al., 2005).

In any event, we speculate that maintenance of a physiological ratio of the two isoforms (estimated to 1/4, Long/Short Oskar; A.E., unpublished data) is crucial to stimulate the clathrin-mediated endocytosis. Consistent with this, overexpressing Long Oskar in wild-type oocytes also induces an alternative, non-clathrin-dependent endocytic pathway (data not shown), confirming that the balance of expression of the two Oskar isoforms is critical.

In contrast to Long Oskar, whose sublocalization agrees with a function in endocytosis, it is not obvious how Short Oskar could directly regulate endocytosis and/or Long Oskar function. We detected only residual membrane association of Short Oskar in transgenic oocytes expressing this isoform alone. However, it is possible that Long Oskar enhances this association in wild-type oocytes. In this hypothesis, Short Oskar might interact functionally with the endocytic membrane to directly regulate either endocytosis or Long Oskar activity. Alternatively, Short Oskar might act indirectly by promoting local concentration of critical regulators of clathrin-mediated endocytosis at the posterior pole, possibly dependent on polar granule assembly. Further investigation of the specific function of Short Oskar in endocytosis will require the development of molecular tools circumventing the requirement for Long Oskar in Short Oskar expression and localization.

A Model for Polar Granule Maintenance at the Posterior Pole

Long Oskar is required for efficient maintenance of Short Oskar at the posterior pole of the oocyte (Vanzo and Ephrussi, 2002). Our finding that Short Oskar largely accumulates in polar granules during oogenesis therefore implies that Long Oskar is essential for polar granule maintenance or integrity. Polar granules are only transiently found in close proximity to endocytic membranes on which Long Oskar localizes, when they form at stage 9 (data not shown). Then, as they mature from stage 9 to stage 10, they become larger, denser, and move away from the area where endocytosis occurs, to accumulate more internally at the edge of the endocytic zone (Figure 1B). This observation suggests that polar granules are not maintained at the posterior pole by direct anchoring to the endocytic membranes.

The cortical F-actin cytoskeleton has previously been implicated in posterior anchoring of Oskar in oocytes (Jankovics et al., 2002; Polesello et al., 2002; Babu et al., 2004), but the mechanism by which it acts was not addressed. In light of our present results, an attractive hypothesis is that polar granule anchoring involves the F-actin projections that we observe at the posterior pole of wild-type oocytes. These projections would be of sufficient length to span the first micrometer internally from the plasma membrane and to contact the underlying polar granules. In addition, they become detectable from stage 10 onward (data not shown), when anchoring is required. These projections are largely reduced in *oskar* null oocytes. As Long Oskar expression per se does not restore their formation, our model suggests the existence of a positive feedback loop mechanism of maintenance, in which polar granules, possibly in concert with Long Oskar, could enhance their own anchoring at the posterior pole.

Endocytosis and Long Oskar Maintenance at the Posterior Pole

In light of the subcellular localization of Long Oskar, its unique competence to anchor at the posterior of the oocyte is quite notable. Interestingly, in addition to its well-documented role in nutrient uptake, endocytosis has emerged as a mechanism restricting the localization of proteins to plasma membrane subdomains in different polarized cells. In yeast, polarized exocytosis coupled with local endocytic recycling localizes membrane proteins at growing shmoo tips (Valdez-Taubas and Pelham, 2003). More recently, endocytic trafficking has been shown to localize epithelial polarity proteins and restrict membrane receptor-dependent signaling during cell migration (Lu and Bilder, 2005; Jékely et al., 2005). By analogy, Long Oskar might be maintained and concentrated by continuous endocytic cycles at the posterior pole. By upregulating endocytosis, Oskar might promote its own accumulation, in addition to that of other membrane-associated factors, at the posterior pole. Consistent with this, Oskar has been shown to enhance the posterior accumulation of Rab11, a small GTPase recruited to endocytic

membranes and required for endocytic recycling in the oocyte (Dollar et al., 2002).

In addition to being actin dependent (see above), Oskar anchoring also relies on an uncharacterized actin-independent mechanism (Babu et al., 2004). This mechanism was inferred from the observation that drug-induced F-actin depolymeriation caused only mild Oskar-anchoring defects in wild-type, in vitro-cultured oocytes (Babu et al., 2004). In light of our findings, we propose that endocytosis might be this alternative mechanism. Consistent with this, the posterior localization of a Long Oskar reporter construct is essentially unaffected by actin depolymerization (referred to as Osk-βGal by Babu et al. [2004]). Significant Oskar-anchoring defects are provoked by F-actin depolymerization in *homer* mutant oocytes (Babu et al., 2004). Although the molecular function of Homer in anchoring is unknown, the authors proposed that the protein is a key player in the actin-independent anchoring mechanism. Strikingly, using IEM, we have observed that a fraction of Homer associates with endocytic membranes and partially colocalizes with Long Oskar-containing endocytic structures (C.R., N.V., and A.E., unpublished data). This observation supports a role of Homer and endocytosis in the mechanism of Long Oskar maintenance.

In conclusion, our work has revealed unexpected cellular functions of Oskar. Beyond its known functions in posterior patterning and germline induction, Oskar regulates asymmetry in clathrin-mediated endocytosis and F-actin organization in the *Drosophila* oocyte. We propose that, by regulating these two cellular processes, in positive feedback loops, Oskar isoforms promote their own maintenance at the posterior pole, thus reinforcing oocyte polarity.

EXPERIMENTAL PROCEDURES

Drosophila Stocks and Transgenes

The wild-type control stock was Oregon R. The *oskar* protein null alleles (osk^{54}, osk^{84}), which were molecularly characterized by Kim-Ha et al. (1991) and $Df(3R)p^{XT103}$, which uncovers *oskar*, were described by Lehmann and Nüsslein-Volhard (1986). Construction of the P(*oskM1R*) transgene, expressing only Short Oskar, and of the P(*oskM139L*) transgene, expressing Long Oskar alone, are described by Vanzo and Ephrussi (2002) and Markussen et al. (1995), respectively.

Antibodies

To generate the anti-Long Oskar antibody (anti-M1M2), a PCR fragment covering the two first translation initiation codons of *oskar* (encoding the 139 aa long M1M2 peptide described by Gunkel et al. [1998]) was cloned in pCALc (Pharmacia). The recombinant peptide was expressed in *Escherichia coli*, purified, and used as antigens for polyclonal antibody production in four mice. The serum was directly used for IEM and immunofluorescence at a 1:1000 dilution. Specificity of the antibody was confirmed (see Figure S1). Other antibodies used in this study, the polyclonal rabbit anti-Oskar antibody recognizing the two isoforms (Vanzo and Ephrussi, 2002), the rat anti-Vasa (Tomancak et al., 1998), the three rabbit antisera (a, b, and c) raised against the oocyte yolk proteins (described by Warren and Mahowald [1979]; Trougakos et al. [2001]; and Butterworth et al. [1999], respectively), the rat anti-Yolkless (Schonbaum et al., 2000), and the anti-clathrin heavy chain serum, have been described elsewhere. Secondary antibodies for immunofluorescence were purchased from Jackson Immunoresearch laboratories.

Immunofluorescence and F-Actin Staining

Ovaries from 2- to 3-day-old females were dissected in Grace's media (GIBCO-BRL). For immunodetection, ovaries were fixed in 4% paraformaldehyde (EM grade) in PBS. After washing in PBS and PBS supplemented with 0.3% Triton X-100, the ovaries were incubated in PBS-1% Triton X-100 and blocked in PBS-2% BSA. The samples were then incubated overnight at 4°C with the primary antibodies and TRITC-coupled phalloidin (Sigma, 1/1000) or phalloidin-SR101 (FluoProbes, 1/300) in the same BSA blocking buffer. The ovaries were rinsed and incubated in the same buffer with fluorescently coupled secondary antibodies (1/300) at room temperature, washed, mounted in Vectashield (Vector Laboratories), and observed with a Leica TCS confocal microscope by using the 63 lens and the x2-6 zoom.

Immuno-Electron Microscopy

Ovaries were fixed in 4% paraformaldehyde and processed as described by Herpers and Rabouille (2004). Alternatively, semi-thick cryosections of 500 nm were cut, collected on glass slides, labeled with anti-yolk protein antibody, and observed by light microscopy, by using the Leica TSC confocal microscope, as described by Sommer et al. (2005).

FM4-64 Uptake

FM4-64 (Molecular Probes) was dissolved in DMSO and used at the final concentration of 10 mM. Ovaries were incubated 5 min, then washed for 15/20 min in PBS, as described by Sommer et al. (2005). Oocytes were directly visualized with a Leica confocal microscope.

Quantitation/Stereology

Distribution of Oskar on the Different Compartments at the Posterior Pole

The posterior pole is defined in the text. The compartments of the posterior pole that were evaluated are the polar granules, the endocytic membrane, and the cytoplasm. The cytoplasm corresponds to the space between the endocytic membrane and the polar granules, where no identifiable structures are observed. The endocytic membrane was defined as Yolkless-positive structures. The different categories of membranes taken into account are the plasma membrane (excluding clathrin-coated areas), clathrin-coated structures, non-coated vesicles and tubules, and sorting endosomes (schematized in Figure 2D). Each gold particle was assigned to a compartment (Ncomp). The total number (Ntotal) is expressed as 100%, and the relative distribution is calculated as Ncomp/Ntotal × 100.

Measurement of Yolk Volume in the Cytoplasm

This measurement was performed by using the point hit method (Rabouille, 1999). Briefly, ultrathin or semi-thick sections were cut and labeled (when appropriate, by using the anti-YPs serum from Trougakos et al. [2001]), as described above. A series of points spaced by 0.5 cm was used to count the number of points falling on the yolk granules (Pyolk) and on the cytoplasm (Pcyto). In this instance, the oocyte cytoplasm was defined as the entire volume comprised within the plasma membrane (including the yolk granules). The yolk granules were defined, either as dense and round objects of typical morphology in EM or as Yolk-positive, round objects in light microscopy. The percentage of cytoplasm occupied by the yolk granules is expressed as Pyolk/Pcytoplasm. This analysis was performed on at least 10 electron- or immunofluorescence micrographs, taken at the magnification of 6000 and 2000, respectively.

Size of the Endocytic Compartment

The volume occupied by endocytic structures within the cytoplasm beneath 10 μm of plasma membrane (for references) was measured by using the point hit method (see above). Electron micrographs showing the plasma membrane and underlying cortex (either at the posterior pole or laterally) of stage-10 wild-type and *oskar* null oocytes were

taken at a final magnification of 54,000. The membrane of endocytic structures (positive for Yolkless) was drawn. Sorting endosomes and condensing yolk granules were excluded from this quantitation. The volume contained within the membrane was estimated by using a series of points spaced by 0.3 cm.

Plasma membrane length was estimated on the same pictures by the intersection method by using a grid whose lines were spaced by 0.3 cm (Rabouille, 1999). The results are expressed as "μm^2 of endocytic compartment/10 μm of plasma membrane." At least 15 micrographs corresponding to each different genetic background and antibody labeling were used.

Total Amount of Yolk Protein in Endocytic Structures

Using micrographs similar to those described above but labeled for yolk protein, the number of gold particles corresponding to yolk present in the endocytic compartment (as defined and drawn above, that is, excluding sorting endosomes and condensing yolk granules) was estimated. The results are expressed as "number of gold particles/10 μm of plasma membrane."

Supplemental Data

Supplemental Data include four figures and one table and are available at http://www.developmentalcell.com/cgi/content/full/12/4/543/DC1/.

ACKNOWLEDGMENTS

We thank Elly van Donselaar for initial EM observations and for help with cryosectioning; Anthony Mahowald, Ioannis Trougakos, and Mary Bownes for their gift of antibodies; and Dominique Morello for helpful discussion and providing conditions and support for the conclusion of this work. C.R. is the recipient of the ZonMw grant from the Nederlandse Organisatie voor Wetenschappelijk Onderzoek (912-04-009). N.V. was supported by a long-term fellowship from the Human Frontier Science Programme and by the Centre National de la Recherche Scientifique.

Received: May 3, 2006
Revised: January 8, 2007
Accepted: March 2, 2007
Published: April 9, 2007

REFERENCES

Babu, K., Cai, Y., Bahri, S., Yang, X., and Chia, W. (2004). Roles of Bifocal, Homer, and F-actin in anchoring Oskar to the posterior cortex of *Drosophila* oocytes. Genes Dev. *18*, 138–143.

Breitwieser, W., Markussen, F.-H., Horstmann, H., and Ephrussi, A. (1996). Oskar protein interaction with Vasa represents an essential step in polar granule assembly. Genes Dev. *10*, 2179–2188.

Butterworth, F.M., Burde, V.S., Mauchline, D., and Bownes, M. (1999). A yolk protein mutant leads to defects in the secretion machinery of *Drosophila melanogaster*. Tissue Cell *31*, 212–222.

DiMario, P.J., and Mahowald, A.P. (1987). Female sterile (1) *yolkless*: a recessive female sterile mutation in *Drosophila melanogaster* with depressed numbers of coated pits and coated vesicles within the developing oocytes. J. Cell Biol. *105*, 199–206.

Dollar, G., Struckhoff, E., Michaud, J., and Cohen, R.S. (2002). Rab11 polarization of the *Drosophila* oocyte: a novel link between membrane trafficking, microtubule organization, and *oskar* mRNA localization and translation. Development *129*, 517–526.

Engqvist-Goldstein, A.E., and Drubin, D.G. (2003). Actin assembly and endocytosis: from yeast to mammals. Annu. Rev. Cell Dev. Biol. *19*, 287–332.

Ephrussi, A., and Lehmann, R. (1992). Induction of germ cell formation by *oskar*. Nature *358*, 387–392.

Ephrussi, A., Dickinson, L.K., and Lehmann, R. (1991). *oskar* organizes the germ plasm and directs localization of the posterior determinant *nanos*. Cell *66*, 37–50.

Gunkel, N., Yano, T., Markussen, F.-H., Olsen, L.C., and Ephrussi, A. (1998). Localization-dependent translation requires a functional interaction between the 5′ and 3′ ends of *oskar* mRNA. Genes Dev. *12*, 1652–1664.

Hay, B., Jan, L.Y., and Jan, Y.N. (1988). A protein component of *Drosophila* polar granules is encoded by *vasa* and has extensive sequence similarity to ATP-dependent helicases. Cell *55*, 577–587.

Herpers, B.H.A., and Rabouille, C. (2004). mRNA localization and ER based protein sorting mechanisms dictates the usage of tER-Golgi units involved in Gurken transport in *Drosophila* oocytes. Mol. Biol. Cell *15*, 5306–5317.

Illmensee, K., and Mahowald, A.P. (1974). Transplantation of posterior polar plasm in *Drosophila*. Induction of germ cells at the anterior pole of the egg. Proc. Natl. Acad. Sci. USA *71*, 1016–1020.

Jankovics, F., Sinka, R., Lukacsovich, T., and Erdelyi, M. (2002). Moesin crosslinks actin and cell membrane in *Drosophila* oocytes and is required for Oskar anchoring. Curr. Biol. *12*, 2060–2065.

Jékely, G., Sung, H.H., Luque, C.M., and Rorth, P. (2005). Regulators of endocytosis maintain localized receptor tyrosine kinase signaling in guided migration. Dev. Cell *9*, 197–207.

Kessell, I., Holst, B.D., and Roth, T.F. (1989). Membranous intermediates in endocytosis are labile, as shown in a temperature-sensitive mutant. Proc. Natl. Acad. Sci. USA *86*, 4968–4972.

Kim-Ha, J., Smith, J.L., and Macdonald, P.M. (1991). *oskar* mRNA is localized to the posterior pole of the *Drosophila* oocyte. Cell *66*, 23–35.

Kim-Ha, J., Kerr, K., and Macdonald, P.M. (1995). Translational regulation of *oskar* mRNA by Bruno, an ovarian RNA-binding protein, is essential. Cell *81*, 403–412.

Kirchhausen, T. (2002). Clathrin adaptors really adapt. Cell *109*, 413–416.

Kirkham, M., Fujita, A., Chadda, R., Nixon, S.J., Kurzchalia, T.V., Sharma, D.K., Pagano, R.E., Hancock, J.F., Mayor, S., and Parton, R.G. (2005). Ultrastructural identification of uncoated caveolin-independent early endocytic vehicles. J. Cell Biol. *168*, 465–476.

Lehmann, R., and Nüsslein-Volhard, C. (1986). Abdominal segmentation, pole cell formation, and embryonic polarity require the localized activity of *oskar*, a maternal gene in *Drosophila*. Cell *47*, 141–152.

Lu, H., and Bilder, D. (2005). Endocytic control of epithelial polarity and proliferation in *Drosophila*. Nat. Cell Biol. *7*, 1232–1239.

Mahowald, A.P. (1962). Fine structure of pole cells and polar granules in *Drosophila melanogaster*. J. Exp. Zool. *151*, 201–215.

Markussen, F.-H., Michon, A.-M., Breitwieser, W., and Ephrussi, A. (1995). Translational control of *oskar* generates Short OSK, the isoform that induces pole plasm assembly. Development *121*, 3723–3732.

Polesello, C., Delon, I., Valenti, P., Ferrer, P., and Payre, F. (2002). Dmoesin controls actin-based cell shape and polarity during *Drosophila melanogaster* oogenesis. Nat. Cell Biol. *4*, 782–789.

Rabouille, C. (1999). Quantitative aspect of immunogold in embedded and non embedded sections. In Methods in Molecular Biology, Vol. 117: Electron Microscopy Methods and Protocols, N. Hajibagheri, ed. (Totowa, NJ: Humana Press), pp. 125–147.

Rongo, C., Gavis, E.R., and Lehmann, R. (1995). Localization of *oskar* RNA regulates *oskar* translation and requires Oskar protein. Development *121*, 2737–2746.

Schonbaum, C.P., Perrino, J.J., and Mahowald, A.P. (2000). Regulation of the vitellogenin receptor during *Drosophila melanogaster* oogenesis. Mol. Biol. Cell *11*, 511–521.

Sommer, B., Oprins, A., Rabouille, C., and Munro, S. (2005). The exocyst component Sec5 is present on endocytic vesicles in the oocyte of *Drosophila melanogaster*. J. Cell Biol. *169*, 953–963.

Tomancak, P., Guichet, A., Závorszky, P., and Ephrussi, A. (1998). Oocyte polarity depends on regulation of *gurken* by Vasa. Development *125*, 1722–1732.

Trougakos, I.P., Papassideri, I.S., Waring, G.L., and Margaritis, L.H. (2001). Differential sorting of constitutively co-secreted proteins in the ovarian follicle cells of *Drosophila*. Eur. J. Cell Biol. *80*, 271–284.

Tsuruhara, T., Koenig, J.H., and Ikeda, K. (1990). Synchronized endocytosis studied in the oocyte of a temperature-sensitive mutant of *Drosophila melanogaster*. Cell Tissue Res. *259*, 199–207.

Valdez-Taubas, J., and Pelham, H.R.B. (2003). Slow diffusion of proteins in the yeast plasma membrane allows polarity to be maintained by endocytic cycling. Curr. Biol. *13*, 1636–1640.

Vanzo, N.F., and Ephrussi, A. (2002). Oskar anchoring restricts pole plasm formation to the posterior of the *Drosophila* oocyte. Development *129*, 3705–3714.

Warren, T.G., and Mahowald, A.P. (1979). Isolation and partial chemical characterization of three major yolk polypeptides from *Drosophila melanogaster*. Dev. Biol. *68*, 130–139.